Polymer Chemistry

ROYAL SOCIETY OF CHEMISTRY

PAPER

View Article Online
View Journal | View Issue

Cite this: *Polym. Chem.*, 2026, **17**, 1569

Solubility-limited depolymerization kinetics in the glycolysis of carbonyl-containing polymers

Shelby Watson-Sanders,[a] Kendra Day Johnson,[a] Sarah Barber,[a] Alison Biery,[a] Landri Wilcox,[a] Nicholas J. Galan,[b] Jackie Zheng,[b] Tomonori Saito[b] and Mark Dadmun*[a]

Chemical recycling of condensation polymers is often rationalized on the basis of the intrinsic reactivity of ester and carbonate functional groups. However, under heterogeneous conditions relevant to plastic waste processing and environmental degradation, bulk depolymerization rates often diverge from trends predicted by homogeneous chemistry. Here, we investigate how polymer–solvent compatibility, catalyst strength, and phase behavior govern the heterogeneous glycolysis of carbonyl-containing polymers. Using poly(ethylene terephthalate) (PET), glycol-modified PET (PETG), and bisphenol-A polycarbonate (PC) as model systems, we examine depolymerization kinetics at 180 °C with ethylene glycol and bisphenol A as diols under both amphoteric organosalt (TBD : MSA) and strong base (TBD) catalysis. Despite substantial differences in crystallinity and glycol uptake, PET and PETG depolymerize at comparable rates under organosalt catalysis, while PC depolymerizes significantly more slowly under identical conditions. Time-resolved molecular weight analysis and thermal characterization demonstrate that these rate differences do not arise from crystallinity, swelling, or inherent carbonyl reactivity, but instead reflect solubility-limited kinetics that constrain the transition from heterogeneous to homogeneous reaction regimes. When polymer solubility is low, depolymerization remains heterogeneous and slow; when solubility is enhanced—either through increased polymer–diol compatibility or stronger base catalysis—rapid homogeneous depolymerization is observed, reversing apparent reactivity trends. These results establish solubility and phase behavior as primary determinants of depolymerization kinetics in heterogeneous polymer recycling systems. By demonstrating how catalyst selection and solvent compatibility can expose or overcome solubility limitations, this work provides mechanistic insight to design more energy-efficient and selective chemical recycling processes. More broadly, these findings suggest that polymers with limited solvent or water compatibility may resist chemical degradation in the environment, favoring fragmentation and persistence as micro- and nanoplastics. Understanding solubility-controlled depolymerization offers a pathway toward more sustainable polymer design and end-of-life chemical recovery.

Received 3rd March 2026,
Accepted 6th March 2026

DOI: 10.1039/d6py00219f

rsc.li/polymers

Introduction

An increasing amount of virgin plastic is produced yearly, with 400 million metric tons produced in 2021.[1] After reaching their end-of-life cycle, the destination of these plastics must be more environmentally friendly, as 79% of plastic is discarded in landfills and 12% is incinerated.[1–5] Only 9% of plastic is recycled, mainly through mechanical recycling, which is only feasible for a number of cycles, as it has been shown to degrade the polymer.[1–5] More sustainable manufacturing and recycling processes, including chemical recycling, are essential to decrease reliance on petroleum resources and the volume of polymer waste.[6–8] The design of efficiently recyclable polymers[9–12] will move society towards this goal; however, in parallel, there must be efforts to understand the chemical processes that occur during chemical recycling of current commercially available polymers to develop processes to remediate current waste, as well as provide insight into how to create tomorrow's polymers that are more sustainable.

There is extensive interest in understanding and optimizing the chemical recycling of polyesters and polycarbonates, as the carbonyl group within the polymer chain is reasonably reactive and susceptible to nucleophilic attack.[13,14] For example, investigations have examined the depolymerization of consumer waste polycarbonate (PC), polyethylene terephthalate (PET), polyamide (PA), and polyurethane (PU) *via* glycolysis in the same reaction vial.[1,15] Specifically, in these studies, the

[a]*Chemistry Department, University of Tennessee, Knoxville, TN 37996, USA. E-mail: Dad@utk.edu*
[b]*Oak Ridge National Laboratory, Oak Ridge, TN, USA*

reaction temperature selectivity controlled the polymer that depolymerizes by chain scission. In these studies, PC depolymerizes to monomer at 130 °C, while all other polymers remain intact. Increasing the temperature to 180 °C depolymerizes PET.[1,15] While utilizing reaction temperature to control chain scission of specific polymer chains and their carbonyl groups is impressive and novel, a more thorough understanding of the important parameters that control the rate of depolymerization of polycarbonate and polyesters will offer foundational insight that will guide future design of more readily depolymerized polymers and depolymerization processes.

Cooper *et al.*[16] in 2002 described this specific need, as aromatic PC is more resistant to hydrolytic degradation than aromatic polyesters. However, when both aromatic esters and diaryl carbonates undergo hydrolysis, there isn't a significant preference for acyl substitution of carbonates over esters in acidic and neutral conditions, as there is in basic conditions. Cooper *et al.*[16] observed that the greater resistance to hydrolysis of aromatic polycarbonates compared to polyesters cannot be attributed alone to a higher reactivity of the ester group, where Scheme 1 illustrates the ester and carbonate functional groups of PET and PC, and must also be due to other factors that control the hydrolysis rate of the bulk polymers. It remains unknown whether this trend, where bulk aromatic polycarbonates depolymerize faster than aromatic polyesters, is due to factors such as differences in crystallinity or solvent solubility in polymers. What Cooper *et al.*[16] found was that this difference was not caused by an inherent ease of hydrolysis of one functional group over the other in acidic or neutral conditions.

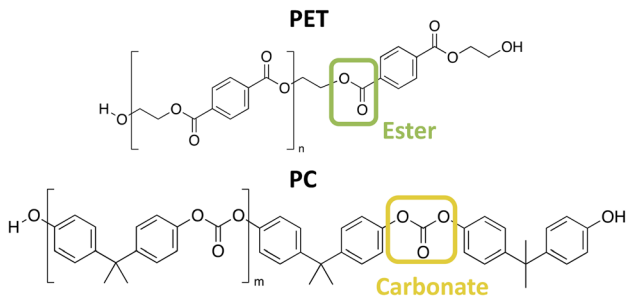

Scheme 1 Ester and carbonate containing polymers, PET and PC, respectively.

Our previous studies show that the depolymerization of PET by glycolysis involves consecutive steps that include the swelling of the PET flake with ethylene glycol (EG), followed by the catalyzed reaction of the hydroxyl group on the EG with the PET ester group in the amorphous part of the semi-crystalline PET.[17] In this view, the penetration of the hydroxyl-containing reactant (ethylene glycol in this case) into the PET solid, and the reaction of the hydroxyl and carbonyl are important consecutive steps in the process.

An additional important aspect of this research program revolves around the nature of the heterogeneous reaction as the reaction progresses. At the beginning of the reaction, the reaction is heterogeneously catalyzed as the polymer flake remains as a solid. As the reaction progresses, some depolymerized polymer product becomes soluble in the diol, while some polymer remains insoluble. Thus, at this stage, there are coexisting homogeneously catalyzed reactions of the soluble species and heterogeneously catalyzed reactions of the insoluble polymer. Finally, at the latest stages of the depolymerization, the polymer may be sufficiently depolymerized to be completely soluble in the diol, and thus the reaction is homogeneously catalyzed. These three stages are illustrated in Fig. 1 and are labeled as the heterogeneous stage, coexistence stage,

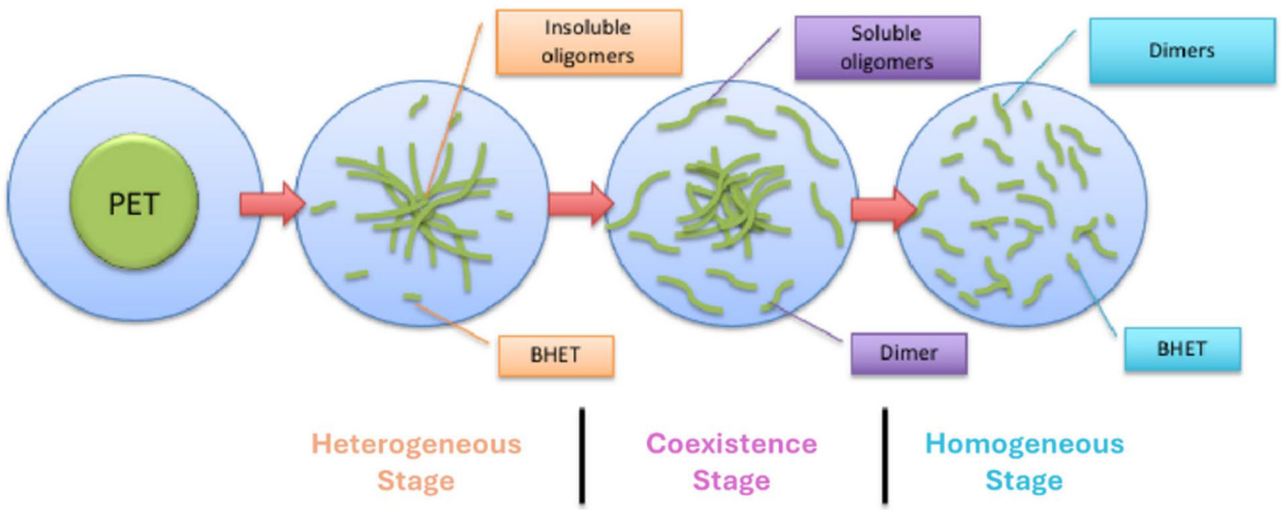

Fig. 1 Illustration of the three stages of heterogeneous depolymerization as described in the text: the heterogeneous stage, the coexistence stage, and the homogeneous stage. The heterogeneous stage occurs when the polymer is not dissolved in the solvent. The coexistence stage involves both dissolved polymer and polymer not dissolved in the solvent. The homogeneous stage occurs when all polymers are dissolved in the solvent.

and homogeneous stage. Clearly, the crystallinity of the polymer and the relative solubility of the diol and polymer will impact the progression of the reaction through these three stages. In fact, the reaction may not reach the homogeneous stage if the depolymerized product is not sufficiently soluble in the diol.

Although Fig. 1 presents a schematic representation of heterogeneous depolymerization, the stage boundaries in this work are defined using objective, experimentally measurable criteria. The heterogeneous stage is identified by retention of polymer flake morphology and recovery of >90% insoluble material after workup, as in our previous work.[17] Transition into the coexistence stage is marked by the appearance of a soluble oligomer fraction, quantified by a decrease in insoluble yield, but insoluble flakes remain present. The homogeneous stage is defined by the complete loss of recoverable insoluble polymer and an optically uniform reaction mixture. These criteria are evaluated using mass balance (soluble *versus* insoluble yield), molecular weight evolution of the soluble and insoluble fractions, and dissolution behavior, as detailed in the SI.

Given this perspective, this study has focused on providing insight into the relative importance of the transport of the glycol (reactant) to the carbonyl and the reactivity of the carbonyl on the observed depolymerization rate. As the transport of the diol to the carbonyl will depend on polymer crystallinity and polymer/diol compatibility, this research program will evaluate the impact of polymer crystallinity, diol-polymer compatibility, and carbonyl reactivity on the rate of heterogeneous depolymerizations to determine the relative importance of each parameter on the reaction progress.

Many studies have monitored the depolymerization of polyethylene terephthalate (PET) or polycarbonate (PC).[18–21] PET is a common plastic, with ~30 million tons produced annually in the U.S.,[4–6,8,22–33] while aromatic PC, used for safety glasses, airplane windows, and helmets, sees about 3 million tons produced yearly.[34,35] Tritan™ copolyester and polyethylene terephthalate glycol (PETG), developed in the last 20 years,[4,5,36] has a PET-like molecular structure but is amorphous, unlike semi-crystalline PET.[36,37] Amorphous polymers are easier to dissolve than crystalline ones, so diols may penetrate PETG and PC more readily than PET.[4,29,38,39] However, the impact of swelling and chemical reactivity on depolymerization rates is not well understood. The literature often refers to the acyl substitution of carbonate groups as transesterification and transcarbonation.[34,35,40,41] For simplicity, in this study, we will refer to the acyl substitution of carbonate groups as transesterification.

Thus, the depolymerization of polyethylene terephthalate (PET), aromatic polycarbonate (PC), and polyethylene terephthalate glycol (PETG) is examined in this study to provide insight into the impact of polymer crystallinity, polymer/diol solubility, and carbonyl reactivity on the rate of depolymerization. These experiments will monitor the depolymerization of these polymers under the same conditions – at 180 °C using Triazabicyclodecene (TBD) and Methanesulfonic acid (MSA) as the organo-salt catalyst,[42,43] using either ethylene glycol (EG) or bisphenol-A (BPA) as reactants. EG and BPA were the diols of choice as EG has a similar chemical structure to part of the polyesters, while the chemical structure of BPA mimics part of the repeat unit of the PC. The swelling of each polymer by each diol is also monitored to provide insight into the relative transport rate of the glycol into the solid polymer.

Experimental methods

Materials

PET was sourced from commercial Coca-Cola bottles, which were washed and cut into squares (8 mm × 5 mm × 0.3 mm). Polycarbonate (PC) was sourced from a PC sheet from Home Depot, which was cut into squares with a Dremel (8 mm × 6 mm × 2.65 mm). Polyethylene terephthalate glycol (PETG) Embrace LV copolyester pellets (2.91 mm × 2.72 mm × 1.92 mm) were provided by Eastman Chemical Company and used as received. 1,5,7-Triazabicyclo[4.4.0]dec-5-ene (98.0+%, TCI America™), Methanesulfonic Acid (99%), Ethylene glycol, (99.8%, anhydrous, AcroSeal™, Thermo Scientific Chemicals), bisphenol-A (BPA), Tetrahydrofuran (THF), methanol, 20 mL vials, 100 mL round bottom flasks, 12.7 × 8 mm stir bars, and 12 × 4.5 mm stir bars were sourced from Fischer Scientific. All chemicals were used as received.

Catalyst

A 1 : 1 mixture of Triazabicyclodecene (TBD) and Methanesulfonic acid (MSA) is used as the organocatalyst to depolymerize the polymers, as has been previously reported.[42,44] The salt catalyst was prepared by mixing TBD and MSA at 1 : 1 molar ratios of acid to base at 80 °C until solidified. The product obtained was a transparent and homogenous solid.[42]

Reaction conditions

Ethylene glycol (EG) reactions. Ethylene Glycol (EG), TBD : MSA catalyst, and a carbonyl-containing polymer (1 g) (such as PC, PET, or PETG) are used in a molar ratio of 20 : 0.5 : 1, respectively, and stir bar were all placed in a 20 mL reaction vial inside a glovebox, sealed with a septum, and transferred outside the glovebox into a 180 °C oil bath. Previous studies indicate that the glycolysis of PET and PC takes 2 hours and 4 hours, respectively, at 180 °C to reach completion.[15,42] To analyze the evolution of the polymer chains during depolymerization, the reaction was stopped at various reaction times, and the products were recovered and characterized as described below.[42] Scheme 2 illustrates the glycolysis of the 3 polymers to isolate oligomers. Previous literature[44–46] has demonstrated that during the glycolysis of PET and PC, there is an increase in hydroxyl and phenol end groups, respectively, as shown in Scheme 2. The ^{1}H NMR spectrum shown in Fig. S1–S3 confirms this with an increased signal from methylene protons at around 4.0 ppm, which corresponds to methylene groups adjacent to hydroxyl end groups. This is consistent with the formation of hydroxyl-ter-

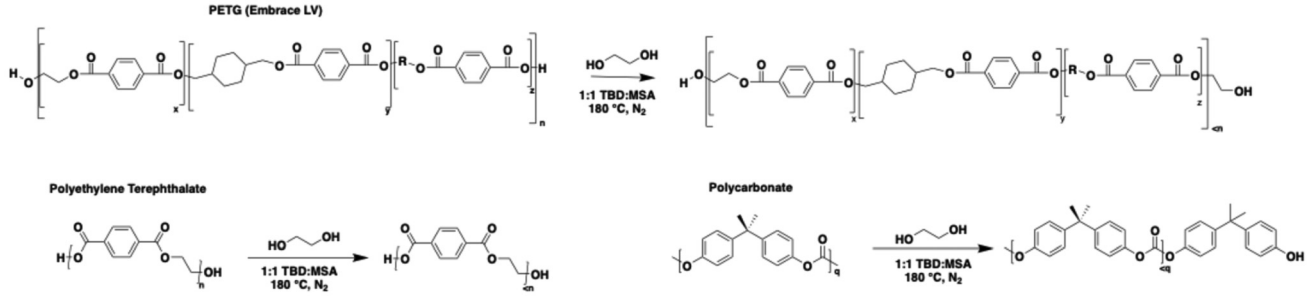

Scheme 2 Heterogeneous glycolysis reaction of PETG (Embrace LV), PET, and PC catalyzed by TBD : MSA to create oligomers.

minated polyester chains. Conversely, when PC is depolymerized with EG, there is a prominent increase in methylene protons linked to BPA-based end groups. This indicates that EG undergoes intramolecular ring-closing more readily to form ethylene carbonate than to retain a hydroxyl end group.[15,45]

EG reaction product workup. After the reaction was allowed to run for a set time, the reaction vials were removed from the oil bath. The ethylene glycol (EG) and depolymerization products that are soluble in EG were decanted from the reaction vials. The remaining solid PC that is insoluble in EG was washed with methanol three times by suspending it in 20 mL of methanol and stirring with a stir bar for 15 minutes. The remaining solid PET or PETG that is insoluble in EG was washed with water three times. After the third wash and decant, the reaction vial containing the EG insoluble materials was set on a 70 °C hotplate overnight to evaporate any remaining methanol or water.

Bisphenol-A (BPA) reactions. Bisphenol-A (BPA), TBD : MSA catalyst, and a carbonyl-containing polymer (1 g) (such as PC, PET, or PETG) were used in a molar ratio of 20 : 0.5 : 1, respectively, and stir bar were all placed in a 100 mL round bottom flask inside a glovebox, sealed with a septa, and transferred outside the glovebox into a 180 °C oil bath. To analyze the evolution of the polymer chains during PC and PET depolymerization, the reaction was stopped at various reaction times, and the products were recovered and characterized as described below. Fig. S1–S3 show ^{1}H NMR to confirm the isolation of BPA-capped oligomers. Depolymerizing both polyesters and polycarbonates with BPA results in an increase in BPA-related end groups across all systems. Notably, PET depolymerized with BPA does not show a rise in the ~4.0 ppm methylene signal associated with α-hydroxyl end groups, suggesting BPA's strong preference for attachment and its dominance as the primary chain-end functionality (Scheme 3).

BPA reaction product workup. After the reaction was allowed to run for a set time, the round bottom flasks were taken from the oil bath. The BPA and polymer mixture were decanted into 200 mL of methanol, as BPA is soluble in methanol, and PC and PET are not. The methanol mixture was vacuum filtered to isolate BPA and methanol insoluble oligomers. After the vacuum filtration, the BPA and methanol insoluble oligomers were set on a 70 °C hotplate overnight to evaporate any remaining methanol. Then, BPA insoluble polymer flakes were separated from the methanol insoluble oligomers. These two oligomers can be separated as the remaining BPA insoluble polymer flakes in the reaction vessel are visible, while the BPA soluble oligomers are not. Upon crashing this reaction mixture into methanol, the BPA soluble oligomers precipitate as powder, as seen in Fig. 2. In Fig. 2, the BPA insoluble oligomers are the remaining polymer flakes highlighted in green, and the methanol insoluble oligomers are the polymer powder highlighted in blue.

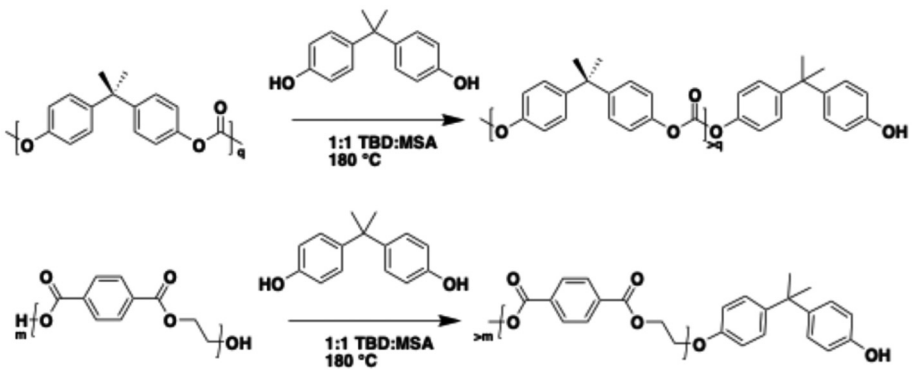

Scheme 3 Heterogeneous PC and PET depolymerization reaction utilizing bisphenol-A (BPA) diol and catalyzed by TBD : MSA to create BPA-capped oligomers.

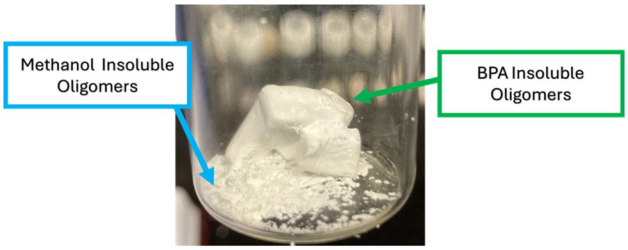

Fig. 2 Picture of the products of polycarbonate (PC) that is depolymerized with BPA for 10 minutes. The BPA insoluble oligomers are noted in green, while the methanol insoluble oligomers are noted in blue.

Depolymerization product characterization

Size exclusion chromatography (SEC). Size-exclusion chromatography determined the molecular weight characteristics of the depolymerization products as a function of reaction time. Molecular weights of PET and PETG depolymerized with ethylene glycol were determined using SEC equipped with absolute detection, allowing direct determination of molecular weight. In contrast, PET depolymerized with bisphenol A and all polycarbonate (PC) samples were analyzed by SEC using conventional calibration standards due to solvent and detector compatibility constraints. As a result, molecular weights reported for BPA-depolymerized PET and PC represent relative values. These data are used to evaluate molecular-weight evolution over reaction time rather than absolute molar mass.

The SEC analyses for PC were completed at the Institute of Advanced Materials and Manufacturing (IAMM) using a THF Gel permeation Chromatograph/Size Exclusion Chromatograph (GPC/SEC). This analysis used a Tosoh EcoSEC GPC system and a refractive index (RI) detector calibrated to polystyrene (PS) standards ranging from 600 Da to 2230 kDa. The column set in the instrument include the following: 2 Tosoh TSKgel SuperMultiporeHZ-M (4.6 × 150 mm and 4 μm) and a TSKgel SuperMultiporeHZ-M guard. The samples were run with a Flow Rate of 0.35 mL min^{-1} and an analysis temperature of 40 °C. PC samples were dissolved in THF overnight at a 1.5 mg mL^{-1} concentration before being filtered (0.2 μm PTFE filter) and placed in the autosampler.

The SEC analyses for PET and PETG depolymerized with EG were completed in 1,1,1,3,3,3-hexafluoroisopropanol (HFIP). This analysis used an Agilent 1260 Infinity II HPLC stack connected with a Wyatt miniDAWN TREOS (MALS) and Wyatt Optilab T-rEX (dRI) detector. A poly(methyl methacrylate) (PMMA) standard and commercial PET substrate were used to verify system performance. Molar mass values were calculated assuming a dn/dc of 0.191 and 0.257 mL g^{-1} for PMMA and PET, respectively. The mobile phase and sample prep used HFIP amended with 20 mM of sodium trifluoroacetate (NaTFAc). The HPLC used 3 Agilent PL HFIPgel 250 × 4.6 mm columns attached in series with a matching guard column. PET and PETG samples were dissolved in HFIP for five days at a ~5 mg mL^{-1} concentration before being filtered (0.2 μm) and placed in the autosampler. The samples were run with a flow rate of 0.35 mL min^{-1} and a column temperature of 40 °C.

The SEC analyses of the depolymerization of PET with BPA were completed at the Oak Ridge National Lab using GPC/SEC. PET samples were dissolved in HFIP for five days. Samples were then filtered through a 0.2 μm syringe filter into an autosampler vial. This analysis was performed on an Agilent 1260 Infinity II LC system equipped with an Agilent MiniMIX-C Guard column (PL Gel 5 μM, 50 × 4.6 mm) and two Agilent PL HFIPgel (250 × 4.6 mm, 9 μm). The mobile phase was HFIP at a flow rate of 0.3 mL min^{-1} (an Agilent EasiVial PMMA standard, containing four discrete molecular weights, was used for calibration). Detection was conducted using a differential refractive index (RI) detector, a light scattering detector with two angles at 90° and 15°. Number-average molecular weights (M_n), weight-average molecular weights (M_w), and dispersities ($Đ = M_w/M_n$) were calculated based on the system calibration and by assuming 100% mass elution from the columns using the Agilent GPC/SEC software.

Intrinsic viscosity of the samples was also measured separately from the SEC analysis to compare and provide an absolute molecular weight of the PET and PETG, the viscosity average molecular weight (M_v). M_v is a comparable average to the weight average molecular weight (M_w).[47] Fig. S4 shows the changes in M_w and M_v across all depolymerization times, demonstrating that the relative molecular weight (M_w) obtained from SEC is similar to the absolute viscosity-average molecular weight (M_v) determined from intrinsic viscosity measurements.

Normalized swelling [%] of polymers by EG. Half a gram of polymer (PET, PETG, or PC) was placed in a 20 mL vial with EG and a stir bar in a 1 : 35 molar ratio of polymer to solvent, where the vial was sealed with a septa. Samples were mixed and heated in a 180 °C oil bath for various times (30, 60, 90, and 135 minutes) following the swelling procedure from Najmi.[29] Swelling times were limited to these times to prevent the dissolution of the polymer into the solvent. After a specific time, the solvent was decanted hot from the vial and rinsed with DI water for 15 minutes. Then, the water was decanted, rinsed again for another 15 minutes, and repeated. The samples were heated at 75 °C for 72 hours to evaporate off the remaining water before being weighed. The mass of the sample was then determined and used to calculate the normalized swelling using eqn (1), where m_f is the final mass, m_i is the initial mass and n_{flakes} is the number of flakes in the sample. The number of flakes was individually counted, following Vlachos *et al.*'s work.[29] Eqn (1) combines the variable swelling ratio of different flakes to obtain the normalized swelling per polymer flake, as the dimensions of the flakes vary between the three polymers of interest.[29,48] Measurements were stopped when the polymer started to dissolve, as demonstrated by a significant decrease in the normalized swelling. The swelling data is plotted *versus* the square root of time, following Vlachos *et al.*'s work.[29]

$$\text{Normalized swelling}\,[\%] = \frac{\frac{m_f - m_i}{m_i}}{n_{flakes}} \times 100 \quad (1)$$

Results & discussion

Starting material characterization

Since Polyethylene Terephthalate Glycol (PETG, Embrace LV), Polyethylene Terephthalate (PET), and Polycarbonate (PC) originate from different sources, PETG from Eastman Chemical Company and PET and PC from consumer waste, the starting molecular weights and crystallinities of the polymers were characterized. The results are presented in Fig. 3 and Fig. S1–S5. Fig. 3 shows the initial molecular weights of all three polymers, while Fig. S1–S3 show the ^{1}H NMR spectra of all three polymers. Fig. S4 shows the initial viscosity molecular weight (M_v) for both PET and PETG, and Fig. S5 presents the DSC curves for PET, PC, and PETG before the depolymerization reaction begins.

According to Fig. 3, PC and PET have similar weight average molecular weights (M_w), represented in light purple, whereas PETG has a lower M_w than both. PET also has the largest number-average molecular weight (M_n), indicated in dark purple, followed by PETG and PC. This indicates that the consumer waste-derived PC exhibits the largest dispersity ($Đ$) among the three starting materials. PET and PETG have comparable dispersities of 1.5 and 1.4, respectively, although they differ in crystallinity. Fig. S5 demonstrates that PET has a crystalline melting peak starting at 240 °C, while PETG and PC do not exhibit a crystalline melting peak, indicating that they are amorphous.

Ethylene glycol depolymerization of PET, PC, and PETG

Both the ester-containing polymers (PETG and PET) and the carbonate-containing polymer (PC) were depolymerized under the same reaction conditions to provide insight into the importance of carbonyl reactivity on the rate of depolymerization. The TBD : MSA organosalt was selected to provide a neutral, thermally stable, amphoteric catalytic environment that enables controlled depolymerization without rapid polymer dissolution, allowing mechanistic interrogation of heterogeneous depolymerization behavior.[42] Fig. 4 shows the changes in the number-average molecular weight (M_n), weight-average molecular weight (M_w), and dispersity ($Đ$) for the EG insoluble fraction of all three polymers as a function of glycolysis reaction time. In Fig. 4(a), the M_n (dark green), M_w (light green), and $Đ$ (black line) of PETG decrease from 27 kDa, 37 kDa, and 1.4 to 6 kDa, 7 kDa, and 1.2, respectively, over a 75-minute reaction period. Meanwhile, Fig. 4(b) reveals that the M_n (dark blue), M_w (light blue), and $Đ$ (purple line) of PET decline from 33 kDa, 49 kDa, and 1.5 to 8 kDa, 10 kDa, and 1.2, respectively, over a 105-minute reaction period.

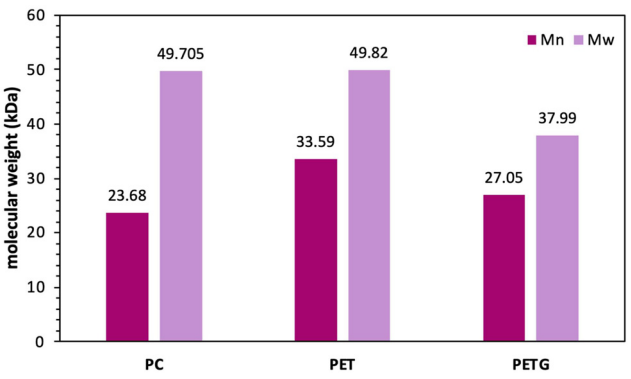

Fig. 3 Molecular weights (M_n, purple; M_w, light purple) of virgin polymers (PC, PET, PETG) before depolymerization.

Interestingly, despite PETG and PET having slightly different initial molecular weights and the fact that PETG is amorphous while PET is semi-crystalline, the depolymerization of both ester-containing polymers occurs at similar rates, resulting in comparable molecular weight oligomers at similar reaction times.

These two polymers have similar chemical structures, chain lengths, and dispersities, yet PET is semi-crystalline while PETG is amorphous.[36,37] The similarity of chain evolution during their depolymerization serves as an initial indication that crystallinity of the polyester does not significantly influence the rate of depolymerization by glycolysis. Furthermore, our previous studies[44] and others have demonstrated that PET depolymerization occurs *via* the reaction of glycol with the ester groups in the amorphous phase, necessitating the transport of glycol throughout the flake.[49,50] As crystalline polymers are more difficult to dissolve than amorphous polymers,[39,51] one might expect the transport of ethylene glycol (EG) into the amorphous phase of PET to be slower than that in PETG. However, given that the rate of depolymerization *via* glycolysis is comparable for both polymers, this data indicates that the transport of glycol to the carbonyl does not control the rate of this depolymerization reaction. The impact of crystallinity on PET glycolysis has been investigated further in our ongoing work on PET samples with systematically varied crystallinity, where we find that increasing the crystalline fraction does not markedly alter the percent reduction in molecular weight under similar depolymerization conditions. This is consistent with the relatively small differences observed here between amorphous and semicrystalline PET.

Fig. 4(c) displays the evolution of molecular weight of PC during depolymerization, plotting M_n (dark orange), M_w (light orange), and $Đ$ (blue line) of PC as a function of reaction time. The data indicate a decrease in M_n and M_w with increased depolymerization time; however, it takes almost four to five times longer to depolymerize PC into oligomers compared to the depolymerization of PET or PETG. Notably, the $Đ$ of the PC oligomers that emerge from the depolymerization initially increases during the first half-hour of the reaction before decreasing at later times, with $Đ$ falling slightly below two after five hours, contrasting the behavior observed in the polyesters. Overall, Fig. 4 shows that bulk PC depolymerizes more slowly than bulk PET or PETG under the same heterogeneous conditions, echoing the longstanding mystery noted in the literature.[16] If diaryl carbonates react faster *via* acyl substitution than aromatic esters in homogeneous systems, what factor, such as carbonyl reactivity, crystallinity, or polymer-solvent

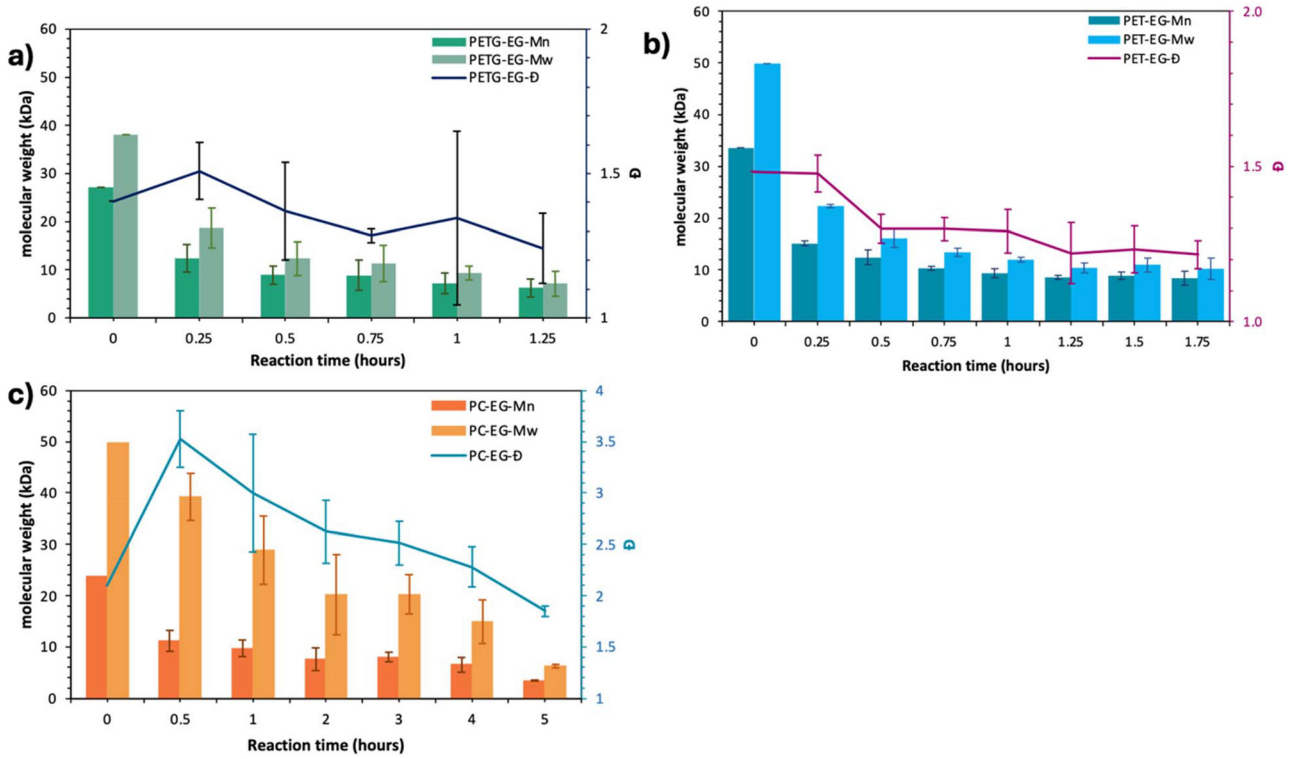

Fig. 4 (a) The change in EG insoluble PETG molecular weight as a function of reaction time: M_n (dark green), M_w (green), and dispersity ($Đ$) (purple). (b) The change in EG insoluble PET chain length as a function of reaction time: M_n (dark blue), M_w (blue), and $Đ$ (purple). (c) The change in EG insoluble PC chain length as a function of reaction time: M_n (orange), M_w (yellow), and $Đ$ (blue).

compatibility, most significantly impacts the reaction rate in Fig. 4?

To contextualize these molecular-weight trends within the phase behavior of the depolymerization system, Fig. S6 examines the evolution of EG-soluble and EG-insoluble oligomer fractions. Under TBD : MSA-catalyzed glycolysis, the majority of oligomeric material for PET, PETG, and PC remains insoluble in EG over much of the reaction, consistent with the heterogeneous conditions targeted in this study. At later reaction times, Fig. S6(b) shows that PET and PETG exhibit increased turbidity and the emergence of partially EG-soluble oligomers, indicating a transition into a heterogeneous–coexistence regime, whereas PC remains largely EG-insoluble. For PET, Fig. S6(c) shows that the molecular weights of both EG-soluble and EG-insoluble oligomers converges at later stages of depolymerization, consistent with partial dissolution of depolymerized chains into the glycol phase. These observations confirm that the molecular-weight evolution discussed above primarily reflects chain scission occurring within the solid polymer phase during early depolymerization.

To evaluate the impact of EG transport on the carbonyl group in the solid polymer on the rate of depolymerization, swelling experiments were conducted. This swelling process is the initial step in polymer dissolution, so discussing this process can provide valuable insights into the importance of glycol transport in the depolymerization process. Polymer dissolution is known to be a multistep process,[9,11–13,51] where the solvent first diffuses into the polymer, causing it to swell. In amorphous polymers, the chains then begin to disentangle and dissolve into the bulk solution. In contrast, the diffusion of the solvent is hindered in crystalline polymers due to confinement by the crystals, which adds an additional step, polymer decrystallization, to the dissolution process.[39] Thus, understanding the rate of swelling in the polymers and, consequently, the transport of EG into the polymer during depolymerization will provide quantitative evidence of the importance of this process on the rate of depolymerization.

Fig. 5 shows the percent swelling per polymer flake as a function of the square root of swelling time, following literature procedure.[29] PETG (green) and PC (orange) absorb ethylene glycol more quickly than PET (blue), where the normalized swelling amounts and rates are quite similar for both amorphous polymers. PET swells to a lesser extent per flake, which we attribute to the inhibition of glycol diffusion into the polymer flake by the PET crystallinity.[39]

Interestingly, despite PETG and PET having similar chemical structures and therefore comparable affinities for EG, their swelling behaviors differ. The rate at which glycol diffuses into PETG is more similar to that of EG diffusing into PC, even though these two have very different chemical structures. Importantly, both PC and PETG are amorphous. Clearly, in these systems, the transport of glycol into the polymer flake is

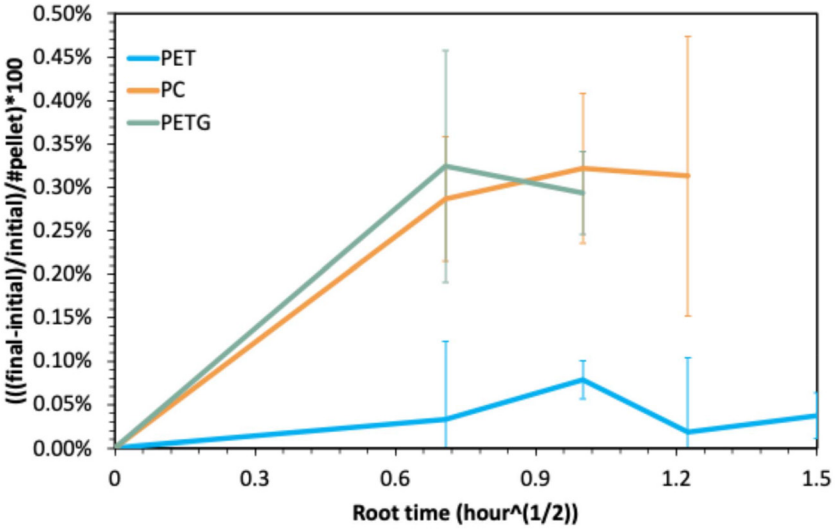

Fig. 5 Normalized swelling per polymer flake of PET (blue), PC (orange), and PETG (green) with EG at 180 °C as a function of the square root of time, following Vlachos *et al.*'s work.[29]

influenced more by the presence or absence of polymer crystals than by the specific affinity between the polymer and glycol. Moreover, both amorphous polymers begin to dissolve at later times in the swelling tests, whereas the semicrystalline polymer (PET) does not. We interpret this to indicate that EG does not disrupt the crystalline structure of PET but merely swells the amorphous phase, as shown in previous studies.[52] The data in Fig. 5 clearly demonstrate that the swelling of the polymer flake by EG is primarily governed by polymer crystallinity and is largely independent of the chemical structure of the polymer in these studies.

Fig. 5 reveals that the amorphous polymers, PETG and PC, swell similarly and more quickly with more glycol than PET. However, PETG and PC do not depolymerize at the same rates, as shown in Fig. 4. Likewise, while PETG absorbs glycol faster than PET, both polymers depolymerize at comparable rates. Put another way, despite the more rapid transport of glycol into PETG than in PET, PETG does not depolymerize more quickly than PET. These results therefore demonstrate that the depolymerization by glycolysis reaction of these polymers is not limited by the diffusion of the glycol to the carbonyl. We interpret the fact that both ester-containing polymers depolymerize faster than the carbonate-containing polymers despite the observed differences in swelling to demonstrate the importance of the reactivity of the carbonyl carbon on the depolymerization reaction, a clear deviation from the simple diaryl carbonate and aromatic ester hydrolysis experiments performed by Cooper *et al.*[16]

To provide more insight into the importance of carbonyl reactivity on depolymerization rates, Fig. 6 plots the percent decrease in M_n and M_w of all three polymers over the course of the depolymerization reaction. Importantly, the goal of employing TBD : MSA was not to maximize depolymerization rate, but to suppress immediate homogenization so that differences in polymer functionality, crystallinity, and solubility could be resolved. Given their different starting molecular weights, this figure provides a clear quantitative overview of the variation in chain length with reaction time for the EG-insoluble depolymerization product. The data in Fig. 6 emphasize that PET and PETG depolymerize at similar rates, as evidenced by the similar decrease in $\%M_w$ (light blue for PET and light green for PETG) and $\%M_n$ (dark blue for PET and dark green for PETG). Interestingly, both PET and PETG show a more rapid decrease in $\%M_w$ relative to $\%M_n$. Since M_w correlates with higher molecular weight polymers in the sample, this suggests that the glycolysis reactions more readily break larger polyester chains than smaller ones.

Fig. 6 also shows that the M_n (dark orange) and M_w (light orange) of PC decrease by 50% within the first hour of the reaction, only reaching 20% of the original molecular weight after 5 hours. In contrast, a similar reduction in chain length for PET and PETG takes approximately 75 minutes of reaction time. Thus, Fig. 6 demonstrates that polymers containing esters depolymerize at a similar rate, regardless of crystallinity, while the polymer with carbonate functionality depolymerizes more slowly than those with ester groups. Interestingly, PC shows a more rapid decrease in $\%M_n$ relative to $\%M_w$ until 5 hours into the reaction when the $Đ$ falls slightly below two. Since M_w correlates with higher molecular weight polymers in the sample, this suggests that glycolysis reactions more readily break shorter polycarbonate chains than larger ones.

A review of the relative reactivity between carbonates and esters provides further fundamental insight into these observations. Notably, literature shows that whether the reaction conditions are acidic, neutral, or basic significantly influences the preference for acyl substitution in esters *versus* carbonates. Under acidic or neutral conditions, esters and carbonates exhibit similar activation energies, resulting in comparable

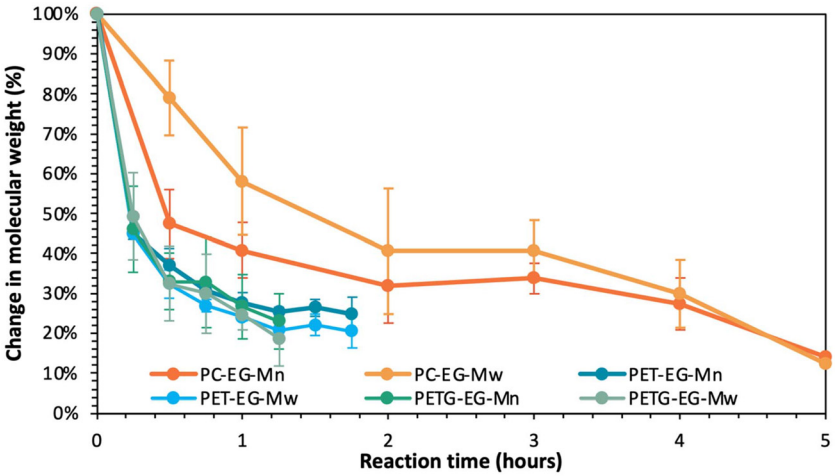

Fig. 6 Change in EG insoluble molecular weight during depolymerization *via* glycolysis as a function of reaction time. Data for PETG: M_n (dark green) and M_w (green); data for PET: M_n (dark blue) and M_w (blue); data for PC: M_n (orange) and M_w (yellow).

favorability for acyl substitution.[16,53,54] However, in basic conditions, studies indicate that even for aromatic esters and carbonates, such as those in our polymers, carbonates favor acyl cleavage more.[16,53,54] The TBD : MSA catalyst mixture used in our experiments likely creates an amphoteric or "buffered" environment, which combines both acidic and basic sites to stabilize proton transfer and promote selective activation at the acyl carbon.[43,55] This balanced catalytic environment facilitates nucleophilic attack on the carbonyl carbon while moderating the basicity or acidity, helping to avoid excessive cleavage reactions at sensitive sites.[55–59] Our reaction in Fig. 6 demonstrates a clear preference for ester over carbonate acyl substitution under neutral catalyst conditions, which deviates from existing literature. To verify these findings, PC was depolymerized for 15 minutes under varying conditions, from acidic to basic. Fig. 7 shows the M_n (blue) and M_w (green) of virgin PC and depolymerized PC under different catalyst conditions, from acidic to neutral to basic (left to right in Fig. 7), using the ratio of TBD (base) to the assumed 1 molar ratio of MSA (acid). This aligns with literature reports: in acidic and neutral conditions, the reactions are similar, while in basic conditions, PC is fully depolymerized to monomer within 15 minutes. Even with an excessive molar excess of acid (0.18 molar excess), there is no significant difference between depolymerization in acidic and neutral conditions. Conversely, even a 0.05 molar excess of base results in a faster reaction rate, significantly different from the 0.01 molar excess of acid. In acidic and neutral settings, the polymer mostly remains undissolved in EG, with molecular weights decreasing by about 41.6% (M_n) and 28.6% (M_w) after 15 minutes, similar to observations in Fig. 6. In contrast, in basic conditions, the polymer dissolves completely and depolymerizes to monomer within the same timeframe. The combined effects of homogeneous reaction conditions and increased reaction rates suggest that further

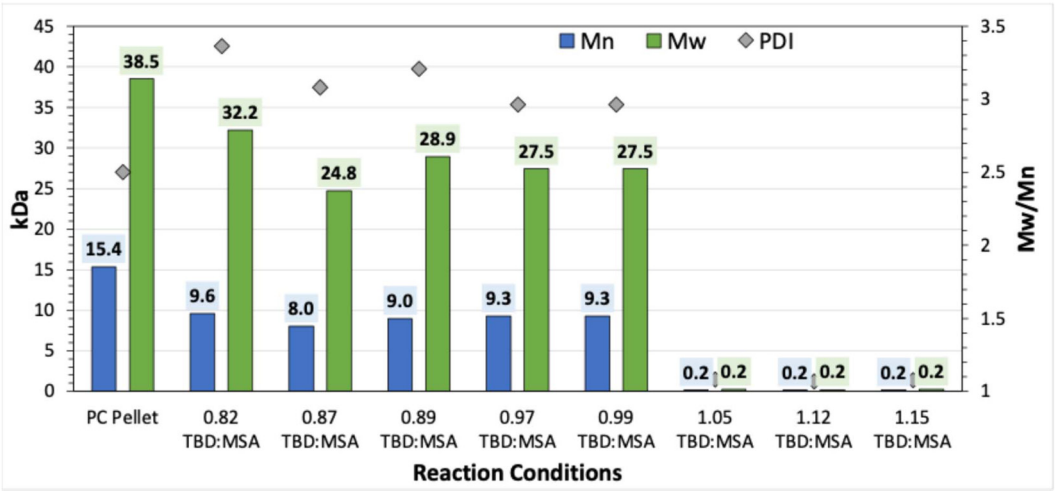

Fig. 7 Change in molecular weight of PC depolymerized for 15 minutes using a salt catalyst with different ratios of acid (MSA) to base (TBDA).

studies in both acidic and basic environments are necessary to fully understand this distinct mechanism.

While carbonates are generally more electrophilic in acidic conditions than in basic ones, this increased electrophilicity did not lead to a faster reaction rate in the acidic pathway shown in Fig. 7.[60–62] Conversely, the resonance-stabilized phenoxide formed under basic conditions acts as a better leaving group than phenol in acidic conditions, thus facilitating depolymerization, as depicted in Fig. 7.[15,34,60,63–67] According to literature reports, similar experiments with polyesters suggest that depolymerization is more favorable in acidic conditions because protonated esters are more electrophilic, and hydroxyl groups are better leaving groups than esters and alkoxides in basic media.[16,53,54,60–62,67,68] Although more research is needed, Fig. S7 shows complete depolymerization of all three polymers using a TBD : MSA catalyst ratio of 1 : 0 under purely basic conditions. Under purely basic conditions (TBD alone), all polymers dissolve within minutes and depolymerize rapidly to monomer, obscuring differences in carbonyl reactivity and phase behavior. As such, TBD alone is unsuitable to probe heterogeneous depolymerization mechanisms. Further investigation is necessary to fully understand the reaction mechanism and rate, but this highlights how solubility influences the depolymerization process.

Overall, the literature and Fig. 7 demonstrate that there should be no difference in favorability for depolymerizing polyesters and polycarbonates under acidic or neutral conditions. However, it would be expected for PC to depolymerize more favorably under basic conditions. Unlike commonly reported acidic or basic catalysts, the TBD : MSA system enables depolymerization to proceed without immediate homogenization, allowing the influence of polymer solubility and functional group chemistry to be resolved. Fig. 6 shows that, despite differences in swelling shown in Fig. 5 (*i.e.*, the abundance of diol at the reaction site), the neutral 1 : 1 TBD : MSA catalyst depolymerizes amorphous and crystalline polyesters similarly and more quickly than polycarbonates.

Depolymerization of PET and PC with Bisphenol-A

To understand how dissolution rate might influence depolymerization, PET and PC were depolymerized using a chemically distinct diol: Bisphenol A (BPA), compared to EG. While EG and BPA differ substantially in physical state, viscosity, concentration, and nucleophilicity, they are used here as contrasting diols to probe the role of polymer–diol compatibility and phase behavior rather than to imply direct kinetic equivalence. PET and PC have solubility parameters ($MPa^{1/2}$) of 20.85 $MPa^{1/2}$ and 22.25 $MPa^{1/2}$, respectively, both with poor solubility in EG (32.98 $MPa^{1/2}$), where a solubility parameter difference greater than 4 $MPa^{1/2}$ indicates poor solubility between polymers and solvent. Consequently, neither polymer dissolved in EG unless assisted by the strong base TBD.[69–74] Since BPA has a solubility parameter of 24.37 $MPa^{1/2}$,[72] it is expected that both PET and PC would be soluble in BPA. This allows for assessing how dissolution impacts the depolymerization rate. Fig. S8 visually illustrates how the polymers' physical forms change when swollen with EG and how both begin to dissolve in BPA. Fig. S9 compares the thickness of the PC flakes as a function of swelling time, showing an increase in size (indicating swelling) with EG and a decrease in size (indicating dissolution) with BPA.

Both an ester-containing polymer (PET) and the carbonate-containing polymer (PC) were also depolymerized with the same reaction conditions, except for using the distinctly different diol, BPA. The depolymerization with BPA was examined to provide additional insight into the importance of the diol-polymer compatibility in the depolymerization process. The results reported above show that the swelling of the polymer flake, inhibited by polymer crystallinity, does not impact the rate of chain scission; thus, the semicrystalline PET continued to be the ester-containing polymer used in this section of the study.

When depolymerizing PET, PC, and PETG in EG, all of the polymer oligomers remained in the heterogeneous stage when using a neutral catalyst, where the polymer remains largely insoluble in the ethylene glycol throughout the reaction as is described in Fig. 1. These observations lead to the conclusion that the depolymerization of PET and PC with BPA does not remain in the heterogeneous stage, as it does when the reaction occurs with ethylene glycol; rather, the reactions quickly transition to the coexistence stage, where some of the product/oligomers are dispersed in the diol, while some are not. Fig. S10 shows the total yield (BPA soluble and insoluble oligomers) and the BPA insoluble oligomer yield of PET and PC over depolymerization time, illustrating a decrease in BPA insoluble oligomers as dissolution into the solvent occurs. Thus, the product of the PC or PET depolymerization in EG retains its solid behavior and flake shape, while those that are depolymerized in BPA do not.

To provide insight into the evolution of the chain structure of the PET and PC depolymerization products in the coexistence or homogeneous stage, SEC analysis offers the molecular weight distribution of BPA soluble and insoluble products. Fig. S11 shows the M_n and M_w of these oligomers during depolymerization as a function of reaction time. The figure indicates these products have substantial chain length. The BPA soluble fraction's molecular weight decreases faster than the insoluble fraction, highlighting reaction acceleration during the shift from heterogeneous to homogeneous stages. To analyze polymer molecular weight over time, the average percent change in M_n and M_w was calculated using eqn (2), which includes terms for yields of insoluble ($n_{insoluble}$) and soluble ($n_{soluble}$) depolymerization oligomers, as well as, molecular weights of insoluble ($M_{t\ insoluble}$) and soluble ($M_{t\ soluble}$) depolymerization oligomers, and the original polymer weight (M_0). Fig. 8 plots the variation in the average molecular weight of both soluble and insoluble fractions of PET M_n (dark blue) and M_w (blue-green), as well as PC M_n (dark orange) and M_w (orange) with reaction time. The overall depolymerization reaction time of both polymers in BPA is shorter than in EG, as PET and PC reach the homogenous stage at 20 minutes and 45 minutes, respectively, when reacting with BPA.

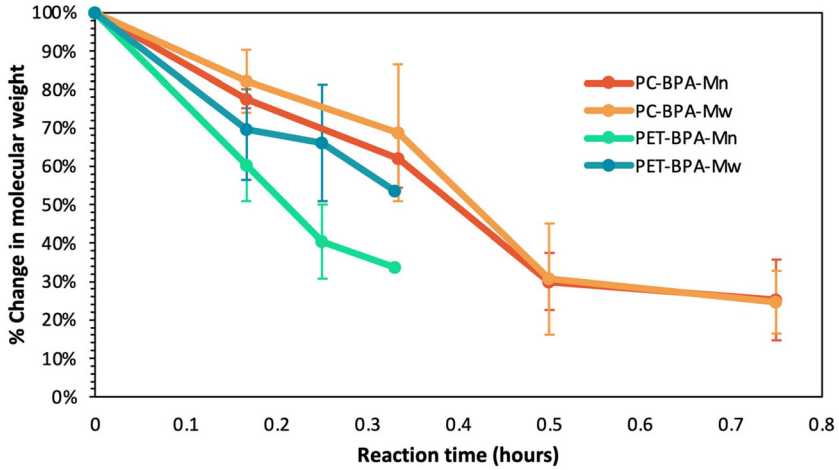

Fig. 8 Change in percent molecular weight for PET and PC with reaction time. It shows the change in molecular weight as a percentage of PET M_n (blue-green), PET M_w (dark blue), PC M_n (dark orange), and PC M_w (orange) with reaction time.

$$\text{Change in average molecular weight [\%]} = \frac{(n_{\text{insoluble}} \times M_{\text{t insouble}}) + (n_{\text{soluble}} \times M_{\text{t soluble}})}{M_0} \times 100 \quad (2)$$

The data in Fig. 8 show that depolymerization reactions using BPA progress more rapidly through the heterogeneous-to-homogeneous transition than those using EG. This behavior arises from the more rapid transition of BPA reactions beyond the heterogeneous stage, as depolymerization proceeds more efficiently in the coexistence and homogeneous stages than in the heterogeneous regime. This observation suggests that the BPA more readily dissolves or disperses the PET and PC depolymerization reaction products.

The dissolution and yield data presented in Fig. S8–S11 provide quantitative, objective validation of the stage boundaries defined in Fig. 1. For example, during BPA depolymerization of PC, the transition from the heterogeneous to coexistence stage coincides with the loss of flake morphology and a sharp decrease in BPA-insoluble yield. This transition is accompanied by a clear inflection in M_n and M_w over time, with the soluble fraction decreasing in molecular weight more rapidly than the insoluble fraction. At longer reaction times, the disappearance of the insoluble fraction and convergence of M_n/M_w behavior indicate transition to the homogeneous stage.

To further probe the origin of this behavior, the swelling of PET and PC in BPA was monitored, as swelling is the first step toward dissolution.[39] Fig. S12 plots the normalized swelling per polymer flake in BPA of PET and PC as a function of swelling time. Fig. S12 indicates that the PET and PC swell more quickly and with more BPA per flake than was observed in their swelling with EG in Fig. 5. Moreover, the PET and PC swell similarly with BPA despite the crystallinity of PET. This is interesting as Fig. 5 demonstrated that the PET crystallinity impacted swelling rates of PC and PET with EG.

Moreover, with a neutral catalyst, EG does not dissolve PET, and thus, decrystallization does not occur. To verify if decrystallization is occurring for PET with BPA, Fig. S13 shows the percent crystallinity of PET with time for different environments, including annealed without a catalyst at the reaction temperature, depolymerized with EG, swelled with EG at the reaction temperature, depolymerized with BPA, and swelled with BPA at the reaction temperature. This data shows that annealing at the reaction temperature without a catalyst or depolymerization/swelling with EG increases the bulk crystallinity of PET. In contrast, the depolymerization/swelling of the PET with BPA decreases the bulk crystallinity, demonstrating that decrystallization of PET occurs with BPA. This variation in solubility can be understood by invoking the Hildebrand solubility parameters of PET, PC, BPA, and EG. PET and PC have solubility parameters ($MPa^{1/2}$) (20.85 $MPa^{1/2}$ and 22.25 $MPa^{1/2}$, respectively) that differ from that of BPA (24.37 $MPa^{1/2}$) by less than 4 $MPa^{1/2}$, while the difference in solubility parameters of PET and PC and that of EG (32.98 $MPa^{1/2}$) is much larger ~ 10–12 $MPa^{1/2}$.[69–74] The similarity of the BPA solubility parameter to that of the polymers indicates that there is a greater affinity of the two polymers to BPA than to EG. Thus, it makes sense that the depolymerization products of both polymers BPA dissolve in BPA more readily, while the depolymerization products do not dissolve in EG. This results in the reactions that occur with EG remaining in the heterogeneous stage, due to the insolubility of the polymers in the EG. Although BPA is a phenolic diol and EG is a primary alcohol with higher intrinsic nucleophilicity, the observed differences in depolymerization behavior under neutral conditions occur prior to full homogenization and therefore primarily reflect differences in polymer solubility rather than intrinsic chemical reactivity.

Holistically, this data shows that polymer–diol affinity governs the apparent depolymerization rate by controlling when the reaction exits the heterogeneous regime, rather than by altering intrinsic bond reactivity alone. However, it is not the transport of the diol into the polymer flake that controls the reaction; instead, the polymer's solubility in the diol controls

the rate at which the reaction passes through the three stages of heterogeneous depolymerization. The more soluble polymer–diol pair will transition from the heterogeneous stage to the homogeneous stage more quickly, increasing the rate of the depolymerization reaction. While many qualitative trends observed here are consistent with classical hydrolytic degradation behavior,[75–78] the use of diols introduces a coupled dependence on swelling, dissolution, and product solubility, which fundamentally alters the apparent depolymerization kinetics under neutral conditions. Additionally, this study demonstrates that basic conditions using strong catalysts, such as TBD, can disrupt intermolecular forces and enhance the solubility of polymers in the diol, accelerating the depolymerization process. This effect was evident in all polymers dissolving in EG within 4 minutes of the reaction, illustrated in Fig. S7, showing the critical role of solubility in determining reaction efficiency.

This study elucidates the impact of polymer crystallinity, the reactivity of carbonyl functional groups, and solvent-polymer compatibility on the rate of the depolymerization of polyesters and polycarbonates. Surprisingly, crystallinity does not greatly impact the rate of depolymerization despite the inhibition of the transport of the diol into the polymer flake by the presence of the polymer crystals. The rapid dissolution of all three polymers in EG, catalyzed with TBD, observed within the first few minutes of the reaction, highlights the overriding influence of solubility over crystallinity in controlling depolymerization rates. This study also shows that ester-containing polymers are more easily chemically recycled than carbonate-containing polymers for acidic or neutral catalysts, even if solvent-polymer compatibility is low. Finally, this study reveals the answer to the decades-long mystery, that the solvent-polymer compatibility has the highest impact on the depolymerization reaction rate by governing when the heterogeneous reaction transitions through the three stages of a heterogeneous depolymerization.

Conclusion

This research explores how polymer-solvent compatibility, catalyst type, polymer crystallinity, and carbonyl reactivity affect the heterogeneous depolymerization of carbonyl-containing polymers. The aim is to improve chemical recycling methods and guide the development of more recyclable materials. Although existing studies show that ester and carbonate bonds have similar acyl substitution reactivity in acidic and neutral homogeneous environments, bulk aromatic polyesters degrade faster than aromatic polycarbonates under similar heterogeneous conditions. To understand this difference, we examined whether factors like carbonyl reactivity, crystallinity, or polymer–diol compatibility influence depolymerization rates.

We studied the glycolysis of PETG, PET, and PC at 180 °C using EG and BPA as model nucleophiles with an organo-salt catalyst (TBD : MSA). While PET and PETG depolymerized at comparable rates despite differences in crystallinity and EG absorption, PC reacted much more slowly under the same conditions. These results suggest that diol transport and polymer crystallinity are not the main factors limiting depolymerization. Instead, we found that the polymer's solubility in the diol is crucial: low solubility keeps the reaction in a slower, heterogeneous state, whereas better solubility facilitates a shift to a faster, homogeneous reaction.

Using a stronger base (TBD), all polymers dissolved quickly in EG, emphasizing how catalyst strength enhances solubility and speeds up depolymerization. Conversely, with TBD : MSA under amphoteric conditions, only BPA enabled a quicker shift to a homogeneous phase, likely due to its higher solubility and compatibility with both ester- and carbonate-based polymers. These findings highlight that solvent-polymer affinity and catalyst basicity are essential for triggering the shift from heterogeneous to homogeneous depolymerization, which determines the overall reaction rate.

Finally, these insights have environmental significance: crystalline polymers with low water solubility may resist natural aqueous catalysis, limiting their breakdown and contributing to persistent micro- and nanoplastic pollution. Understanding how solubility influences depolymerization kinetics can help guide both polymer design and strategies for reducing plastic waste.

Conflicts of interest

The authors declare no competing financial, personal, or professional interests that could have influenced the work reported in this manuscript. The glycol-modified polyethylene terephthalate (PETG) used in this study was supplied by Eastman Chemical Company.

Data availability

The data supporting the findings of this study are available within the article and its supplementary information (SI). Supplementary information: detailed experimental methods, NMR, DSC, and FTIR characterization data, molecular weight analyses (including absolute molecular weight determination and Mark–Houwink analysis), swelling measurements, and extended depolymerization results under amphoteric and basic conditions. See DOI: https://doi.org/10.1039/d6py00219f.

Acknowledgements

This work was supported by the National Science Foundation, Polymers program, Division of Materials Research (DMR-2104982). The SEC analysis and some of the mechanistic discussion were supported by the US Department of Energy, Office of Science, Materials Sciences and Engineering Division.

References

1 M. Arifuzzaman, B. G. Sumpter, Z. Demchuk, C. Do, M. A. Arnould, M. A. Rahman, P.-F. Cao, I. Popovs,

R. J. Davis, S. Dai and T. Saito, Selective deconstruction of mixed plastics by a tailored organocatalyst, *Mater. Horiz.*, 2023, **10**(9), 3360–3368, DOI: 10.1039/d3mh00801k.

2 B. Fox, G. Moad, G. Van Diepen, I. Willing and W. D. Cook, Characterization of poly(ethylene terephthalate) and poly (ethylene terephthalate) blends, *Polymer*, 1997, **38**(12), 3035–3043, DOI: 10.1016/s0032-3861(96)00872-5.

3 N. George and T. Kurian, Recent Developments in the Chemical Recycling of Postconsumer Poly(ethylene terephthalate) Waste, *Ind. Eng. Chem. Res.*, 2014, **53**(37), 14185–14198, DOI: 10.1021/ie501995m.

4 E. C. Company. *2023 Sustainability Report*, 2024. https://www.eastman.com/content/dam/eastman/corporate/en/media-center/resources/eastman-sustainability-report-2023.pdf, accessed 02/25/24.

5 E. C. Company, *2022 Sustainability Report*, 2023. https://www.eastman.com/content/dam/eastman/corporate/en/media-center/resources/eastman-sustainability-report-2022.pdf.

6 D. E. Nikles and M. S. Farahat, New Motivation for the Depolymerization Products Derived from Poly(Ethylene Terephthalate) (PET) Waste: a Review, *Macromol. Mater. Eng.*, 2005, **290**(1), 13–30, DOI: 10.1002/mame.200400186.

7 I. R. Shaikh, Organocatalysis: Key Trends in Green Synthetic Chemistry, Challenges, Scope towards Heterogenization, and Importance from Research and Industrial Point of View, *J. Catal.*, 2014, **2014**, 1–35, DOI: 10.1155/2014/402860.

8 J. Xin, Q. Zhang, J. Huang, R. Huang, Q. Z. Jaffery, D. Yan, Q. Zhou, J. Xu and X. Lu, Progress in the catalytic glycolysis of polyethylene terephthalate, *J. Environ. Manage.*, 2021, **296**, 113267, DOI: 10.1016/j.jenvman.2021.113267.

9 M. Hong and E. Y. X. Chen, Towards Truly Sustainable Polymers: A Metal-Free Recyclable Polyester from Biorenewable Non-Strained γ-Butyrolactone, *Angew. Chem.*, 2016, **128**(13), 4260–4265, DOI: 10.1002/ange.201601092.

10 M. Hong and E. Y. X. Chen, Completely recyclable biopolymers with linear and cyclic topologies via ring-opening polymerization of γ-butyrolactone, *Nat. Chem.*, 2016, **8**(1), 42–49, DOI: 10.1038/nchem.2391.

11 J.-B. Zhu, E. M. Watson, J. Tang and E. Y. X. Chen, A synthetic polymer system with repeatable chemical recyclability, *Science*, 2018, **360**(6387), 398–403, DOI: 10.1126/science.aar5498.

12 C. M. Plummer, L. Li and Y. Chen, Ring-Opening Polymerization for the Goal of Chemically Recyclable Polymers, *Macromolecules*, 2023, **56**(3), 731–750, DOI: 10.1021/acs.macromol.2c01694.

13 J. Otera, *Modern Carbonyl Chemistry*, WILEY-VCH, 2000.

14 K. P. C. Vollhardt and E. N. Shore, *Organic Chemistry; Structure and Functions*, Freeman and Company, 2007.

15 C. Jehanno, J. Demarteau, D. Mantione, M. C. Arno, F. Ruipérez, J. L. Hedrick, A. P. Dove and H. Sardon, Selective Chemical Upcycling of Mixed Plastics Guided by a Thermally Stable Organocatalyst, *Angew. Chem., Int. Ed.*, 2021, **60**(12), 6710–6717, DOI: 10.1002/anie.202014860.

16 G. D. Cooper and B. Williams, Hydrolysis of Simple Aromatic Esters and Carbonates, *J. Org. Chem.*, 1962, **27**(10), 3717–3720, DOI: 10.1021/jo01057a529.

17 S. Watson-Sanders and M. Dadmun, More Efficient Chemical Recycling of Poly(Ethylene Terephthalate) by Intercepting Intermediates, *ChemSusChem*, 2024, **17**, e202301698, DOI: 10.1002/cssc.202301698.

18 Z. Guo, J. Wu and J. Wang, Chemical degradation and recycling of polyethylene terephthalate (PET): a review, *RSC Sustainability*, 2025, **3**(5), 2111–2133, DOI: 10.1039/d4su00658e.

19 E. Barnard, J. J. Rubio Arias and W. Thielemans, Chemolytic depolymerisation of PET: a review, *Green Chem.*, 2021, **23**(11), 3765–3789, DOI: 10.1039/d1gc00887k.

20 S. Zhang, M. Li, Z. Zuo and Z. Niu, Recent advances in plastic recycling and upgrading under mild conditions, *Green Chem.*, 2023, **25**(18), 6949–6970, DOI: 10.1039/d3gc01872e.

21 H. Mitta, L. Li, M. Havaei, D. Parida, E. Feghali, K. Elst, A. Aerts, K. Vanbroekhoven and K. M. Van Geem, Challenges and opportunities in catalytic hydrogenolysis of oxygenated plastics waste: polyesters, polycarbonates, and epoxy resins, *Green Chem.*, 2025, **27**(1), 10–40, DOI: 10.1039/d4gc03784g.

22 V. Sinha, M. R. Patel and J. V. Patel, PET waste management by chemical recycling: a review, *J. Polym. Environ.*, 2010, **18**(1), 8–25.

23 A. B. Raheem, Z. Z. Noor, A. Hassan, M. K. Abd Hamid, S. A. Samsudin and A. H. Sabeen, Current developments in chemical recycling of post-consumer polyethylene terephthalate wastes for new materials production: A review, *J. Cleaner Prod.*, 2019, **225**, 1052–1064, DOI: 10.1016/j.jclepro.2019.04.019.

24 J. Y. Jang, K. Sadeghi and J. Seo, Chain-Extending Modification for Value-Added Recycled PET: A Review, *Polym. Rev.*, 2022, **62**(4), 860–889, DOI: 10.1080/15583724.2022.2033765.

25 C. C. Company, *THE COCA-COLA COMPANY 2022 BUSINESS & SUSTAINABILITY REPORT*. 2022. https://www.coca-colacompany.com/content/dam/company/us/en/reports/coca-cola-business-sustainability-report-2022.pdf#page%3D38, accessed 2023 06/04/23.

26 A. Aguado, L. Martínez, L. Becerra, M. Arieta-Araunabeña, S. Arnaiz, A. Asueta and I. Robertson, Chemical depolymerisation of PET complex waste: hydrolysis vs. glycolysis, *J. Mater. Cycles Waste Manage.*, 2014, **16**(2), 201–210, DOI: 10.1007/s10163-013-0177-y.

27 D. Carta, G. Cao and C. D'Angeli, Chemical recycling of poly(ethylene terephthalate) (pet) by hydrolysis and glycolysis, *Environ. Sci. Pollut. Res.*, 2003, **10**(6), 390–394, DOI: 10.1065/espr2001.12.104.8.

28 G. Colomines, J.-J. Robin and G. Tersac, Study of the glycolysis of PET by oligoesters, *Polymer*, 2005, **46**(10), 3230–3247, DOI: 10.1016/j.polymer.2005.02.047.

29 S. Najmi, B. C. Vance, E. Selvam, D. Huang and D. G. Vlachos, Controlling PET oligomers vs monomers via

microwave-induced heating and swelling, *Chem. Eng. J.*, 2023, **471**, 144712, DOI: 10.1016/j.cej.2023.144712.

30 A. Sheel and D. Pant, Chemical Depolymerization of PET Bottles via Glycolysis, in *Recycling of Polyethylene Terephthalate Bottles*, Elsevier Inc, 2019, pp. 61–84.

31 C. V. G. Silva, E. A. D. Silva Filho, F. Uliana, L. F. R. D. Jesus, C. V. P. D. Melo, R. C. Barthus, J. G. A. Rodrigues and G. Vanini, PET glycolysis optimization using ionic liquid [Bmin]ZnCl3 as catalyst and kinetic evaluation, *Polímeros*, 2018, **28**(5), 450–459, DOI: 10.1590/0104-1428.00418.

32 L. Wang, G. A. Nelson, J. Toland and J. D. Holbrey, Glycolysis of PET Using 1,3-Dimethylimidazolium-2-Carboxylate as an Organocatalyst, *ACS Sustainable Chem. Eng.*, 2020, **8**(35), 13362–13368, DOI: 10.1021/acssuschemeng.0c04108.

33 Q. Yue, C. Wang, L. Zhang, Y. Ni and Y. Jin, Glycolysis of poly (ethylene terephthalate)(PET) using basic ionic liquids as catalysts, *Polym. Degrad. Stab.*, 2011, **96**(4), 399–403.

34 J. H. Kamps, T. Hoeks, E. Kung, J. P. Lens, P. J. McCloskey, B. A. J. Noordover and J. P. A. Heuts, Activated carbonates: enabling the synthesis of differentiated polycarbonate resins via melt transcarbonation, *Polym. Chem.*, 2016, **7**(33), 5294–5303, DOI: 10.1039/c6py00925e.

35 R. L. Snyder, D. J. Fortman, G. X. De Hoe, M. A. Hillmyer and W. R. Dichtel, Reprocessable Acid-Degradable Polycarbonate Vitrimers, *Macromolecules*, 2018, **51**(2), 389–397, DOI: 10.1021/acs.macromol.7b02299.

36 S. Bhagia, K. Bornani, S. Ozcan and A. J. Ragauskas, Terephthalic Acid Copolyesters Containing Tetramethylcyclobutanediol for High–Performance Plastics, *ChemistryOpen*, 2021, **10**(8), 830–841, DOI: 10.1002/open.202100171.

37 D. R. Kelsey, B. M. S. , J. S. Grebowicz and H. H. Chuah, High Impact, Amorphous Terephthalate Copolyesters of Rigid2,2,4,4-Tetramethyl-1,3-cyclobutanediol with Flexible Diols, *Macromolecules*, 2000, **33**, 5810–5818, DOI: 10.1021/ma000223.

38 D. J. Saxon, E. A. Gormong, V. M. Shah and T. M. Reineke, Rapid Synthesis of Chemically Recyclable Polycarbonates from Renewable Feedstocks, *ACS Macro Lett.*, 2021, **10**(1), 98–103, DOI: 10.1021/acsmacrolett.0c00747.

39 B. A. Miller-Chou and J. L. Koenig, A review of polymer dissolution, *Prog. Polym. Sci.*, 2003, **28**(8), 1223–1270, DOI: 10.1016/s0079-6700(03)00045-5.

40 F. Aricò, S. Bravo, M. Crisma and P. Tundo, 1,3-Oxazinan-2-ones via carbonate chemistry: a facile, high yielding synthetic approach, *Pure Appl. Chem.*, 2016, **88**(3), 227–237, DOI: 10.1515/pac-2015-1004.

41 W. B. Kim, U. A. Joshi and J. S. Lee, Making Polycarbonates without Employing Phosgene: An Overview on Catalytic Chemistry of Intermediate and Precursor Syntheses for Polycarbonate, *Ind. Eng. Chem. Res.*, 2004, **43**(9), 1897–1914, DOI: 10.1021/ie034004z.

42 C. Jehanno, I. Flores, A. P. Dove, A. J. Müller, F. Ruipérez and H. Sardon, Organocatalysed depolymerisation of PET in a fully sustainable cycle using thermally stable protic ionic salt, *Green Chem.*, 2018, **20**(6), 1205–1212, DOI: 10.1039/c7gc03396f.

43 C. Jehanno, M. M. Pérez-Madrigal, J. Demarteau, H. Sardon and A. P. Dove, Organocatalysis for depolymerisation, *Polym. Chem.*, 2019, **10**(2), 172–186, DOI: 10.1039/c8py01284a.

44 S. D. Watson-Sanders and M. Dadmun, Evolution of Chain Structure during the Glycolysis of Poly(ethylene terephthalate), *ChemSusChem*, 2024, **17**(23), e202301698, DOI: 10.1002/cssc.202301698.

45 N. J. Galan, I. T. Dishner, B. G. Sumpter, V. Kertesz, N. B. Abdul Rahman, F. Polo-Garzon, Z. Demchuk, T. Saito and J. C. Foster, Upcycling of polyethylene terephthalate to high-value chemicals by carbonate-interchange deconstruction, *Green Chem.*, 2025, **27**(47), 15124–15134, DOI: 10.1039/d5gc03354c.

46 A. J. Spicer, A. Brandolese and A. P. Dove, Selective and Sequential Catalytic Chemical Depolymerization and Upcycling of Mixed Plastics, *ACS Macro Lett.*, 2024, 189–194, DOI: 10.1021/acsmacrolett.3c00751.

47 C. Paul and T. P. L. Hiemenz, *Polymer Chemistry*, CRC Press, 2007.

48 X. Zhou, J. Wang, J. Nie and B. Du, Poly(N-isopropylacrylamide)-based ionic hydrogels: synthesis, swelling properties, interfacial adsorption and release of dyes, *Polym. J.*, 2016, **48**(4), 431–438, DOI: 10.1038/pj.2015.123.

49 T. Yoshioka, N. Okayama and A. Okuwaki, Kinetics of Hydrolysis of PET Powder in Nitric Acid by a Modified Shrinking-Core Model, *Ind. Eng. Chem. Res.*, 1998, **37**(2), 336–340, DOI: 10.1021/ie970459a.

50 S. D. Mancini and M. Zanin, Post Consumer Pet Depolymerization by Acid Hydrolysis, *Polym.-Plast. Technol. Eng.*, 2007, **46**(2), 135–144, DOI: 10.1080/03602550601152945.

51 M. Ghasemi, A. Y. Singapati, M. Tsianou and P. Alexandridis, Dissolution of semicrystalline polymer fibers: Numerical modeling and parametric analysis, *AlChE J.*, 2017, **63**(4), 1368–1383, DOI: 10.1002/aic.15615.

52 H. Li, H. A. Aguirre-Villegas, R. D. Allen, X. Bai, C. H. Benson, G. T. Beckham, S. L. Bradshaw, J. L. Brown, R. C. Brown, V. S. Cecon, J. B. Curley, G. W. Curtzwiler, S. Dong, S. Gaddameedi, J. E. García, I. Hermans, M. S. Kim, J. Ma, L. O. Mark, M. Mavrikakis, O. O. Olafasakin, T. A. Osswald, K. G. Papanikolaou, H. Radhakrishnan, M. A. Sanchez Castillo, K. L. Sánchez-Rivera, K. N. Tumu, R. C. Van Lehn, K. L. Vorst, M. M. Wright, J. Wu, V. M. Zavala, P. Zhou and G. W. Huber, Expanding plastics recycling technologies: chemical aspects, technology status and challenges, *Green Chem.*, 2022, **24**(23), 8899–9002, DOI: 10.1039/d2gc02588d.

53 J. H. Jung, M. Ree and H. Kim, Acid- and base-catalyzed hydrolyses of aliphatic polycarbonates and polyesters, *Catal. Today*, 2006, **115**(1–4), 283–287, DOI: 10.1016/j.cattod.2006.02.060.

54 C. M. Comisar, S. E. Hunter, A. Walton and P. E. Savage, Effect of pH on Ether, Ester, and Carbonate Hydrolysis in

High-Temperature Water, *Ind. Eng. Chem. Res.*, 2008, **47**(3), 577–584, DOI: 10.1021/ie0702882.

55 F. Liguori, C. Moreno-Marrodán and P. Barbaro, Valorisation of plastic waste via metal-catalysed depolymerisation, *Beilstein J. Org. Chem.*, 2021, **17**, 589–621, DOI: 10.3762/bjoc.17.53.

56 G. Eshaq and A. E. Elmetwally, (Mg–Zn)–Al layered double hydroxide as a regenerable catalyst for the catalytic glycolysis of polyethylene terephthalate, *J. Mol. Liq.*, 2016, **214**, 1–6, DOI: 10.1016/j.molliq.2015.11.049.

57 C.-T. Chen, J.-H. Kuo, V. D. Pawar, Y. S. Munot, S.-S. Weng, C.-H. Ku and C.-Y. Liu, Nucleophilic Acyl Substitutions of Anhydrides with Protic Nucleophiles Catalyzed by Amphoteric, Oxomolybdenum Species, *J. Org. Chem.*, 2005, **70**(4), 1188–1197, DOI: 10.1021/jo048363v.

58 C.-T. Chen, J.-H. Kuo, C.-H. Li, N. B. Barhate, S.-W. Hon, T.-W. Li, S.-D. Chao, C.-C. Liu, Y.-C. Li, I. H. Chang, J.-S. Lin, C.-J. Liu and Y. C. Chou, Catalytic Nucleophilic Acyl Substitution of Anhydrides by Amphoteric Vanadyl Triflate, *Org. Lett.*, 2001, **3**(23), 3729–3732, DOI: 10.1021/ol016684c.

59 C.-T. Chen and Y. S. Munot, Direct Atom-Efficient Esterification between Carboxylic Acids and Alcohols Catalyzed by Amphoteric, Water-Tolerant $TiO(acac)_2$, *J. Org. Chem.*, 2005, **70**(21), 8625–8627, DOI: 10.1021/jo051337s.

60 P. Tundo and F. Aricò, Reaction Pathways in Carbonates and Esters, *ChemSusChem*, 2023, **16**(23), e202300748, DOI: 10.1002/cssc.202300748.

61 P. Tundo, M. Musolino and F. Aricò, The reactions of dimethyl carbonate and its derivatives, *Green Chem.*, 2018, **20**(1), 28–85, DOI: 10.1039/C7GC01764B.

62 P. Tundo and M. Selva, The Chemistry of Dimethyl Carbonate, *Acc. Chem. Res.*, 2002, **35**(9), 706–716, DOI: 10.1021/ar010076f.

63 X. C. Tang, M. J. Pikal and L. S. Taylor, *Pharm. Res.*, 2002, **19**(4), 484–490, DOI: 10.1023/a:1015199713635.

64 H. Lee, Effects of temperature, salt concentration, and the protonation state on the dynamics and hydrogen-bond interactions of polyelectrolyte multilayers on lipid membranes, *Phys. Chem. Chem. Phys.*, 2016, **18**(9), 6691–6700, DOI: 10.1039/c5cp08039h.

65 M. Gupta and H. F. Svendsen, Theoretical Study of Temperature dependent Enthalpy of Absorption, Heat Capacity, and Entropy changes for Protonation of Amines and Amino Acid Solvents, *Energy Procedia*, 2014, **63**, 1099–1105, DOI: 10.1016/j.egypro.2014.11.118.

66 J. Maia, J. M. Cruz, R. Sendón, J. Bustos, M. E. Cirugeda, J. J. Sanchez and P. Paseiro, Effect of amines in the release of bisphenol A from polycarbonate baby bottles, *Food Res. Int.*, 2010, **43**(5), 1283–1288, DOI: 10.1016/j.foodres.2010.03.014.

67 D. H. R. Dave Evans, *pKa's of Inorganic and Oxo-Acids*, ACS Organic Division, 2024, https://organicchemistrydata.org/hansreich/resources/pka/pka_data/evans_pKa_table.pdf, accessed 2024.

68 H. Wang, An accurate theoretical study of energy barriers of alkaline hydrolysis of carboxylic esters, *Res. Chem. Intermed.*, 2012, **38**(9), 2175–2190, DOI: 10.1007/s11164-012-0535-8.

69 TESTS, A. D. *Surface Free Energy Components by Polar/Dispersion and Acid—Base Analyses; and Hansen Solubility Parameters for Various Polymers*. https://www.accudynetest.com/polytable_02.html, accessed.

70 A. Y. Kwok, G. G. Qiao and D. H. Solomon, Synthetic hydrogels 3. Solvent effects on poly(2-hydroxyethyl methacrylate) networks, *Polymer*, 2004, **45**(12), 4017–4027, DOI: 10.1016/j.polymer.2004.03.104.

71 J. Sun, L. Wang, S. Ding, X. Sun and L. Xu, Solubility Behavior and Thermodynamic Analysis of Bisphenol A in 14 Different Pure Solvents, *J. Chem. Eng. Data*, 2020, **65**(5), 2846–2858, DOI: 10.1021/acs.jced.0c00166.

72 C. M. Hansen, *Hansen Solubility Parameters*. 2007. DOI: 10.1201/9781420006834.

73 *Polymer Handbook*, ed. J. Brandrup, E. H. Immergut and E. A. Grulke, John Wiley & Sons, Inc.: New York, 4th edn, 1999.

74 C. M. Hansen, The Universality of the Solubility Parameter, *Product R&D*, 1969, **8**(1), 2–11, DOI: 10.1021/i360029a002.

75 M. M. Brette, A. H. Holm, A. D. Drozdov and J. D. C. Christiansen, Pure Hydrolysis of Polyamides: A Comparative Study, *Chemistry*, 2023, **6**(1), 13–50, DOI: 10.3390/chemistry6010002.

76 S. F. Yost, P. M. Guirguis, P. Pereira, P. E. Savage and B. D. Vogt, Nanoplastics in Depolymerization Products from Hydrolysis of Poly(Ethylene Terephthalate) in the Solid State, *Macromol. Rapid Commun.*, 2026, **46**, e202500776, DOI: 10.1002/marc.202500776.

77 D. Osei, L. Gurrala, A. Sheldon, J. Mayuga, C. Lincoln, N. A. Rorrer and A. R. C. Morais, Subcritical CO_2–H_2O hydrolysis of polyethylene terephthalate as a sustainable chemical recycling platform, *Green Chem.*, 2024, **26**(11), 6436–6445, DOI: 10.1039/d3gc04576e.

78 K. Ikenaga, T. Inoue and K. Kusakabe, Hydrolysis of PET by Combining Direct Microwave Heating with High Pressure, *Procedia Eng.*, 2016, **148**, 314–318, DOI: 10.1016/j.proeng.2016.06.442.